
Mode-Locked Laser Systems: Theoretical Models

G. H. C. New

Phil. Trans. R. Soc. Lond. A 1980 **298**, 247-256

doi: 10.1098/rsta.1980.0248

Email alerting service

Receive free email alerts when new articles cite this article - sign up in the box at the top right-hand corner of the article or click [here](#)

To subscribe to *Phil. Trans. R. Soc. Lond. A* go to: <http://rsta.royalsocietypublishing.org/subscriptions>

Mode-locked laser systems: theoretical models

BY G. H. C. NEW

Optics Section, Department of Physics, Imperial College, London SW7 2BZ, U.K.

After a short review of the general methods of achieving mode-locked laser operation, the discussion concentrates on the case of passive mode-locking. Rate equation techniques applicable to both giant-pulse and quasi-continuous lasers are outlined. For the giant-pulse case, a sophisticated version of the ‘fluctuation model’ is described, which allows the stochastic features in the mode-locking performance to be examined quantitatively for the first time. Optimization procedures for these lasers are considered. For quasi-continuous lasers, the powerful compression mechanism that is responsible for the efficient generation of subpicosecond pulses in continuous wave (c.w.) dye lasers is described.

1. INTRODUCTION

There are two principal methods of achieving mode-locked laser operation, active and passive.

(i) *Active mode-locking.* An element driven from an external high frequency generator is inserted into the cavity, the frequency being precisely synchronized to the inverse cavity transit time. Acousto-optical or electro-optical devices can be employed for this purpose, providing amplitude modulation or phase modulation (Siegman & Kuizenga 1974). Highly sophisticated actively controlled oscillators offer excellent reliability and are therefore suitable for generating the seed pulses for large amplifier chains (*Laser Focus* 1977). A special case of active mode-locking, currently important for dye lasers, occurs when the pumping source for the laser is another laser that is itself already mode-locked (Bradley *et al.* 1969; Chan & Sari 1974; Frigo *et al.* 1977). If the criterion is the shortness of the pulses ultimately produced, this is usually the most successful active scheme (Ferguson *et al.* 1978); it can also be extended to include more than two lasers operating in cascade (Heritage & Jain 1978).

(ii) *Passive mode-locking.* In this case, mode-locking is achieved through the action of an intra-cavity saturable absorber without any external intervention. The method has the virtue of simplicity and is extremely effective for the generation of ultra-short pulses in quasi-continuous lasers such as dye lasers (Ippen *et al.* 1972; New 1974; Ruddock & Bradley 1976; Diels *et al.* 1978). In most giant pulse lasers, passive mode-locking, though widely used, is inherently unreliable (Wilbrandt & Weber 1975; New 1978, 1979). Considerable success has, however, recently been achieved with combined active–passive mode-locking arrangements (Kishida & Yamane 1976; Tomov *et al.* 1976, 1977; Seka & Bunkenburg 1978).

An important theoretical technique that is applicable to both actively and passively mode-locked systems is the self-reproducing pulse (s.r.p.) method (Creighton & Jackson 1971; Haus 1975 *a, b, c*). A single pulse, assumed already to be present in the cavity, is subjected in turn to passages through the laser medium, the modulator or saturable absorber, and finally an appropriate dissipative element. A solution for the pulse profile is based on the requirement that it undergoes no net change as a result of the sequence of events. Physically, this usually amounts to balancing spectral narrowing, which tends to broaden the pulse profile, against compression effects resulting from the action of the mode-locking device (Creighton & Jackson

1971; Siegman & Kuizenga 1974). An important feature of the s.r.p. method is that the ultimate pulse duration is predicted. In rare circumstances (Ausschnitt 1977), the evolution of the profile towards the final steady state can also be followed.

2. RATE EQUATION ANALYSIS OF PASSIVELY MODE-LOCKED LASERS

Detailed discussion of the s.r.p. technique can be found in the references cited and it will not be treated in this paper. Instead, attention will be directed towards rate equation methods applicable to passively mode-locked laser systems; the widely differing situations obtaining in giant-pulse and quasi-continuous lasers are considered in §§3 and 4 respectively. While rate equation techniques have obvious limitations, they have the merit of simplicity and so offer greater physical insight into the mechanisms of the mode-locking process than more sophisticated methods.

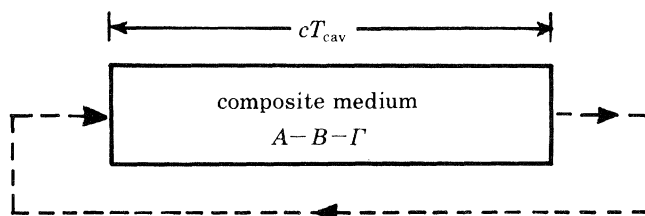


FIGURE 1. Schematic diagram of the ring cavity model. The ring is uniformly filled with a composite medium whose net gain is $(A - B - \Gamma)$ (New 1974).

For the very simple ring cavity model shown schematically in figure 1, the three rate equations describing the propagation of the optical signal through the composite amplifying and absorbing medium are

$$\left(\frac{\partial}{\partial k} + \frac{\partial}{\partial l}\right) F = F(A - B - \Gamma); \quad (1)$$

$$T_{\text{cav}}^{-1} \frac{\partial A}{\partial k} = \left(\frac{A_u - A}{T_{1a}}\right) - A\sigma_a F; \quad (2)$$

$$T_{\text{cav}}^{-1} \frac{\partial B}{\partial k} = \left(\frac{B_u - B}{T_{1b}}\right) - B\sigma_b F. \quad (3)$$

In these equations, T_{cav} is the cavity transit time, $k = t/T_{\text{cav}}$, $l = z/cT_{\text{cav}}$, F is the photon flux, A is the amplification coefficient, B is the saturable absorption coefficient and Γ is the dissipative loss coefficient (all per transit), and A_u and B_u are the unsaturated values of A and B ; T_{1a} and T_{1b} are the respective relaxation times for A and B , while σ_a and σ_b are the respective transition cross sections. It is convenient to define $s = \sigma_b/\sigma_a$ and $P = A_u/(B_u + \Gamma)$. The parameter P is a measure of the pumping level, with $P = 1$ corresponding to the threshold for lasing. Although not explicitly included in the definition of s , it should be noted that the effective value of this parameter is also a function of the beam areas in the absorbing and amplifying media (New 1974).

Equations (1) to (3) possess a steady-state solution for the photon flux F_s , which can be found from the quadratic equation (New *et al.* 1976)

$$\frac{A_u}{1 + \sigma_a T_{1a} F_s} - \frac{B_u}{1 + \sigma_b T_{1b} F_s} - \Gamma = 0. \quad (4)$$

A clearcut distinction between the quasi-continuous and the giant-pulse régimes for a passively mode-locked laser can be based on whether or not (4) represents a state of stable equilibrium. The mathematical conditions defining the two cases have been derived by New & Rea (1976). In practice, the result can be expressed approximately by saying that F_s will be a stable solution if $T_{\text{cav}} \gtrsim T_{1a}$ (quasi-continuous system) but will be unstable if $T_{\text{cav}} \ll T_{1a}$ (giant-pulse system). This is of course exactly the criterion determining whether or not, in the absence of a saturable absorber, the laser Q-switches effectively.

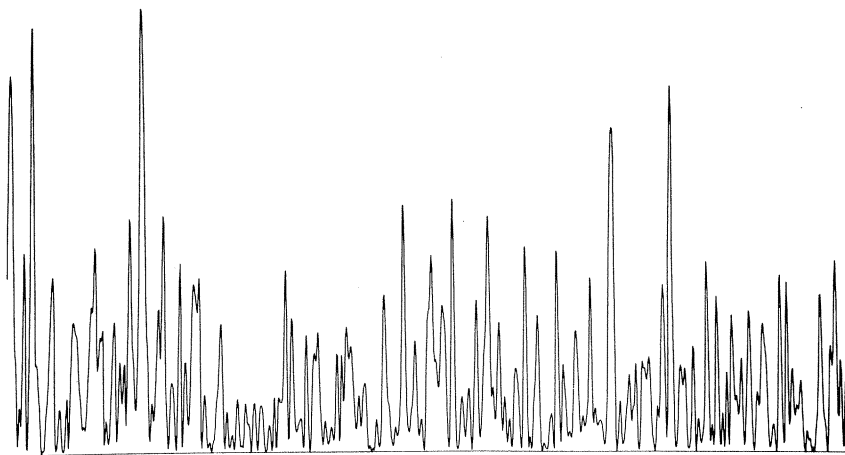


FIGURE 2. Computer simulation of a random multimode laser signal.

3. PASSIVELY MODE-LOCKED GIANT-PULSE LASERS

Numerous authors have studied the dynamics of passively mode-locked giant-pulse lasers over the past decade or so (see Kryukov & Letokhov (1972) and Zel'dovich & Kuznetsova (1972) for early review articles). Most of the work has been based on the so-called 'fluctuation model', according to which the random multimode signal in the laser cavity at the beginning of the mode-locking process (see figure 2) is viewed as a collection of separate fluctuations whose individual histories are then traced under the influence of absorber saturation and amplifier depletion. Since $T_{1a} \gg T_{\text{cav}}$ in typical systems (e.g. neodymium and ruby lasers), the steady state of (4) is never approached and, indeed, the whole giant pulsing event takes place within a time span that is substantially shorter than T_{1a} . This means that the first term on the right hand side of (2) can be discarded. It is also traditional to make the 'inertialess absorber approximation' in which T_{1b} is assumed to be short compared with the duration of the individual fluctuations, so that the equilibrium solution of (3) can be utilized. With these restrictions, and defining $\mu_n = \sigma_b T_{1b} F_n$ as the normalized peak flux of the n th fluctuation, (1)–(3) reduce to (New 1979)

$$\frac{d\mu_n}{dk} = \mu_n \{ \bar{A} - B_u(1 + \mu_n) - \Gamma \}; \quad (5)$$

$$\frac{d\bar{A}}{dk} = -\bar{A}\bar{\mu}T_{\text{cav}}/sT_{1b}. \quad (6)$$

Here \bar{A} ($= A_u$ initially) is the amplification coefficient averaged through the cavity and $\bar{\mu}$ is the mean value of μ in the noisy signal.

Up to about 1973, it was commonly believed that the onset of absorber saturation occurred long before amplifier depletion had any significant effect. If this is the case, then (6) can be ignored and (5) enables the final peak intensity ratio of any two pulses in the pattern to be related to their initial ratio. In particular, for the largest two pulses whose initial ratio may be defined as $r = \mu_1/\mu_2$, it is easy to show that the final value is given by the formula

$$r_f = (r)^{1/Y}, \quad (7)$$

where $Y = G_u/B_u$ and $G_u (= A_u - B_u - \Gamma)$ is the initial (unsaturated) net gain coefficient. The parameter r is a random variable whose statistical properties can be calculated (Glenn 1975, New 1979). Equation (7) suggests that however small r may happen to be, the final ratio r_f can be made as large as desired simply by operating close to threshold so that Y is sufficiently small. As will shortly become apparent, however, as Y is reduced the effects of amplifier depletion that have been neglected in the derivation of (7) become increasingly important in relation to the effects of absorber saturation. It is in any case now generally recognized that the most desirable régime of operation is where the two processes are delicately counterpoised (Chekalin *et al.* 1974; Lariontsev & Serkin 1974; Glenn 1975; Wilbrandt & Weber 1975). To investigate the nature of this balance in detail, the fluctuation structure of the signal is temporarily ignored and μ_n replaced by $\bar{\mu}$ in (5). By writing $\bar{\mu} \sim \exp(G_u k)$, (6) can be integrated and the condition sought under which the depletion of A just offsets the saturation of B in (5) to first order. The result is (New & O'Hare 1978)

$$x \equiv \frac{G_u B_u s T_{1b}}{T_{1a}(B_u + \Gamma + G_u)} = 1. \quad (8)$$

This defines the so-called 'second threshold' (Caruso *et al.* 1973) of the passively Q-switched system, the requirement for Q-switching being $x > 1$. The generalized form of (8) in simultaneous Q-switching and mode-locking is (New 1978, 1979)

$$X \equiv Rx \equiv \frac{RG_u B_u s T_{1b}}{T_{1a}(B_u + \Gamma + G_u)} = X_Q (\approx 0.7), \quad (9)$$

where $R = \mu_1/\bar{\mu}$ with μ_1 the normalized peak intensity of the largest pulse in the fluctuation pattern, and X_Q is a number that has to be determined empirically. Analysis of the linear stage of the signal development, which lasts from the laser threshold until the time when nonlinearity becomes significant (Kryukov & Letokhov 1972; Zel'dovich & Kuznetsova 1972), enables G_u in (9) to be expressed in terms of the system parameters through the formula (New 1979)

$$G_u \approx 11.7 \{P(P-1)\}^{\frac{1}{4}} \{(B_u + \Gamma) T_{cav}/T_{amp}\}^{\frac{1}{2}}, \quad (10)$$

where T_{amp} is a measure of the length of the pumping pulse. Optimum mode-locking occurs when X in (9) slightly exceeds X_Q , in which case histories of the type seen in frame (a) of the computer simulations in figure 3 are obtained. Although in this frame, r (defined as in (7)) only just exceeds unity, the delicate balance between the opposing nonlinear mechanisms ensures that the largest pulse is ultimately many orders of magnitude more intense than any of the rest; the actual value of r_f is much greater than (7) would predict. Unfortunately R , like r , is also a random variable, ranging typically from shot to shot between 3 and 10. It is consequently impossible to guarantee that X is only slightly in excess of X_Q on every occasion. If X falls short of the critical value, a failed shot will be recorded as in frame (c) of figure 3; on the other hand, if X is substantially greater than X_Q , as in frame (d) of the figure, there will be a tendency for double pulsing to occur, particularly if $(r-1)$ chances to be small at the same time.

These considerations lie at the root of the inherent irreproducibility of passively mode-locked giant-pulse systems. The parameters R and r are responsible for virtually all the stochastic features in the performance of these lasers; the overall pattern of events can be discerned in figure 4 where the (r, R) coordinates in 100 computer shots are recorded and the outcome in each case indicated in terms of the proportion of the total energy contained in the dominant pulse. Optimization procedures are summarized in figure 5 where the parameter variations enabling the operating point in the X - Y plane to be shifted in the desirable direction are shown (New 1978, 1979). While the problems can be minimized in this way, there appears to be no way of eliminating shot-to-shot variations completely without going over to a combined active-passive scheme (Kishida & Yamane 1976; Tomov *et al.* 1976, 1977; Seka & Bunkenburg 1978).

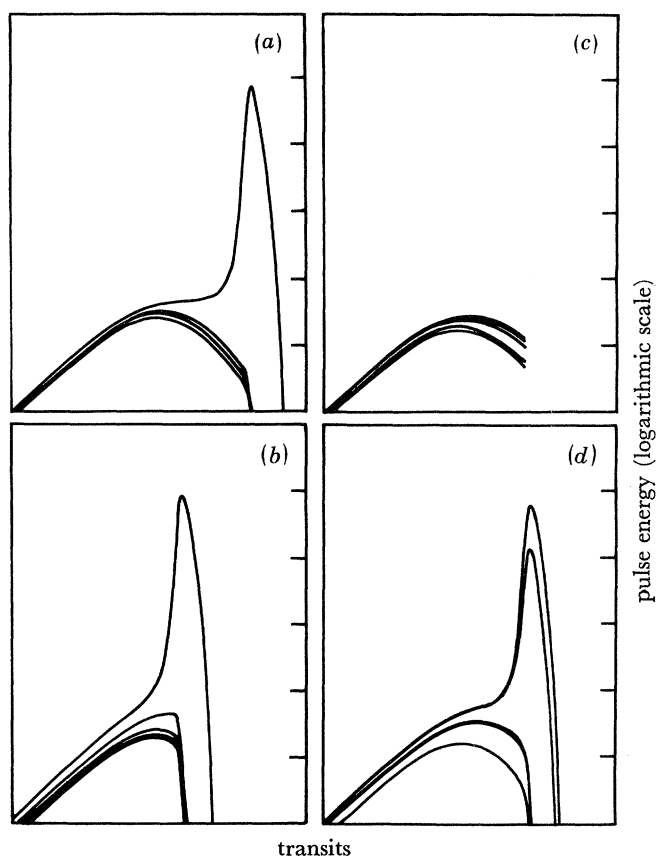


FIGURE 3. Four computer-simulated shots of a passively mode-locked Nd:YAG laser showing the histories of the largest five pulses in the fluctuation pattern (New 1978, 1979). The shots differ only in the structure of the initial random pattern.

4. PASSIVELY MODE-LOCKED QUASI-CONTINUOUS LASERS

Although in a quasi-continuous laser the steady state of (4) is stable in the sense explained in §2, instabilities marking the incipient onset of mode-locking may still develop as soon as spatial variations of F along the cavity axis are admitted into the rate equation mathematics. These can be studied by conducting a linear perturbation analysis on the steady state (Risken & Nummedal 1968; Garside & Lim 1973; New & Rea 1976; New *et al.* 1976), which enables

conditions for the instability of perturbations of different types to be obtained. The boundary between the stable and unstable region in the $P - T_{cav}/T_{1a}$ plane for the lowest harmonic perturbation (one cycle within the cavity) is shown in figure 6. The initial evolution of a ripple of this kind for an operating point to the left (the unstable side) of the boundary is presented in figure 7 (New & Rea 1976).

A more useful approach to the mode-locking problem, particularly when T_{1b} is not too small, is to study the final situation in which a single short pulse ($\tau \ll T_{1a}, T_{1b}$) has already developed,

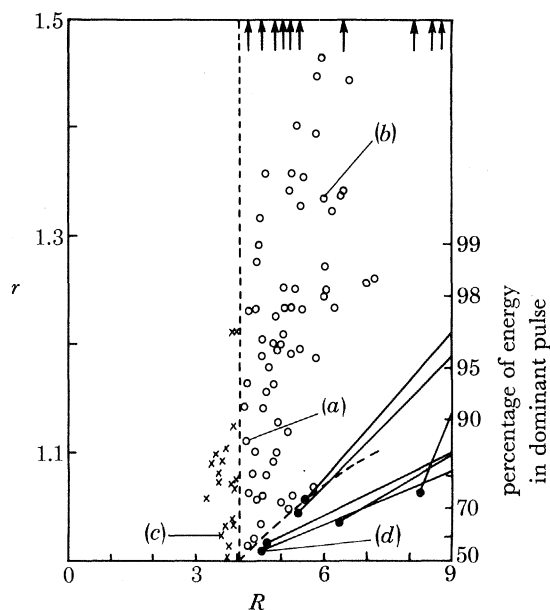


FIGURE 4. Record of 100 computer-simulated shots displayed in terms of the (r, R) coordinates of the initial fluctuation pattern. The shots corresponding to the four frames detailed in figure 3 are indicated. The vertical dotted line marks the second threshold of the system (the value of R that satisfies the identity of (9)). The 20 shots lying to the left of the line are failures (see frame (c) of figure 3). The shots represented by solid dots show a tendency towards double pulsing (e.g. frame (d) in figure 3) and the links to the right-hand axis indicate the percentage of the energy ultimately contained in the dominant pulse. For the open-circled shots, this percentage exceeded 98%.

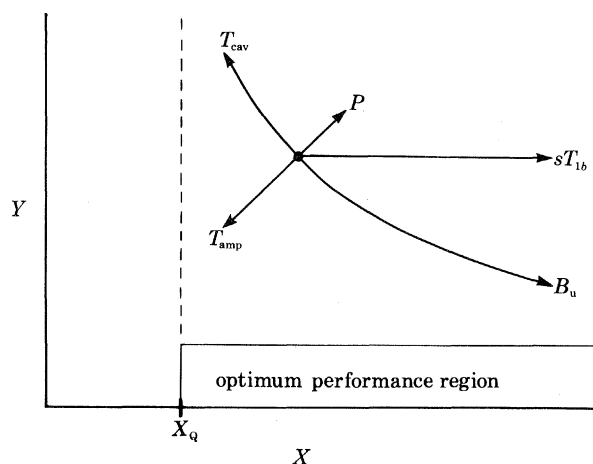


FIGURE 5. Optimization diagram showing the effect of doubling the various parameters and parameter combinations.

A steady-state property exists in this case involving the energy per unit area of the pulse conveniently defined through the formula

$$j = \sigma_a \int_{-\infty}^{+\infty} F(\tau') d\tau'. \quad (11)$$

It is readily shown from the rate equations that j is the root of the equation (New 1974; New *et al.* 1976)

$$A_L(j) - A_T(j) - \{B_L(j) - B_T(j)\}/s - Ij = 0, \quad (12)$$

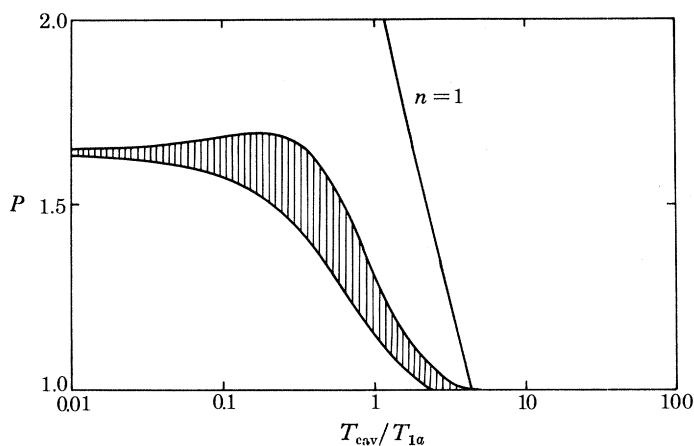


FIGURE 6. The $n=1$ line divides the region to the left where the lowest harmonic perturbation to the steady state of a quasi-continuous laser is unstable and will therefore grow (see figure 7), from the region to the right where this type of perturbation will decay (New & Rea 1976; New *et al.* 1976). Pulse compression of the kind illustrated in figures 8 and 9 occurs inside the hatched region (New 1974; New *et al.* 1976).

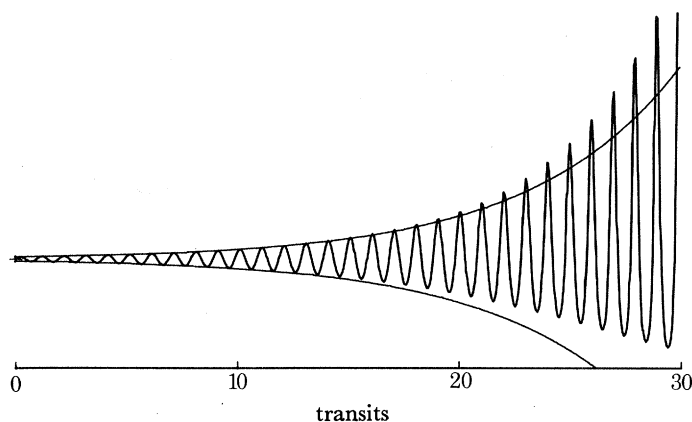


FIGURE 7. Evolution of the lowest harmonic perturbation at an operating point to the left of the $n=1$ boundary in figure 6 (New & Rea 1976).

where the subscripts L and T denote the values of A and B presented to the leading and trailing edges on the pulse respectively. It is easy to show from (2) and (3) (discarding the recovery terms) that

$$A_T(j) = A_L(j) \exp(-j); \quad (13)$$

$$B_T(j) = B_L(j) \exp(-sj), \quad (14)$$

while the requirement that in the steady-state situation A_T and B_T must recover to A_L and B_L in the transit time T_{cav} leads to

$$A_L(j) = A_u \{1 - \exp(-T_{cav}/T_{1a})\} / \{1 - \exp(-j) \exp(-T_{cav}/T_{1a})\}; \quad (15)$$

$$B_L(j) = B_u \{1 - \exp(-T_{cav}/T_{1b})\} / \{1 - \exp(-sj) \exp(-T_{cav}/T_{1b})\}. \quad (16)$$

Once j is found from (12)–(16), the values of the net transmission coefficients $G_L (= A_L - B_L - \Gamma)$ and $G_T (= A_T - B_T - \Gamma)$ for the leading and trailing edges of the pulse profile can be calculated. The most important case is where G_L and G_T are simultaneously negative, implying that the profile will be powerfully compressed while the energy parameter j remains constant; a schematic representation of this process is shown in figure 8. The necessary conditions for the compression process to occur are (New *et al.* 1976)

$$s > 1 + \Gamma/B_u \quad \text{and} \quad T_{1b}/T_{1a} < 1. \quad (17)$$

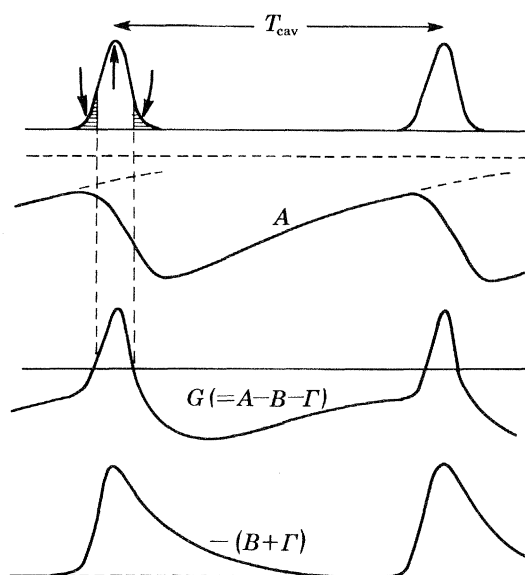


FIGURE 8. Schematic representation of the pulse compression process in a passively mode-locked quasi-continuous laser. The combined action of the two 'slow' saturation processes results in a net loss on both the leading and trailing edges of the mode-locked pulse, but a net gain near the centre.

In addition, T_{cav}/T_{1a} must fall in a limited range near unity, the precise values depending on the pumping parameter P and on the other parameter values. It was in fact the chance coincidence of T_{1a} for Rhodamine 6G and typical cavity transit times that led to the early experimental generation of picosecond and subpicosecond pulses in passively mode-locked dye lasers.

The compression region is shown hatched in figure 6; various other boundaries can be added to this diagram associated with higher pulse multiplicities, and these have been studied in detail by New *et al.* (1976). A sequence of frames showing a numerical simulation of the complete mode-locking process for an operating point inside the compression zone is presented in figure 9. The chief disadvantage of the rate equation approach is that the pulse in the final frame of this figure is moving towards a singularity so that, as previously mentioned, no direct information can be obtained about the final pulse duration. Qualitatively, however, one is

justified in arguing that the more powerful the compression process, the shorter the pulses generated will be. Outside the hatched region in figure 6, a very much weaker 'dynamic' compression process operates (New *et al.* 1976), and substantially longer pulses may therefore be expected to evolve under these conditions.

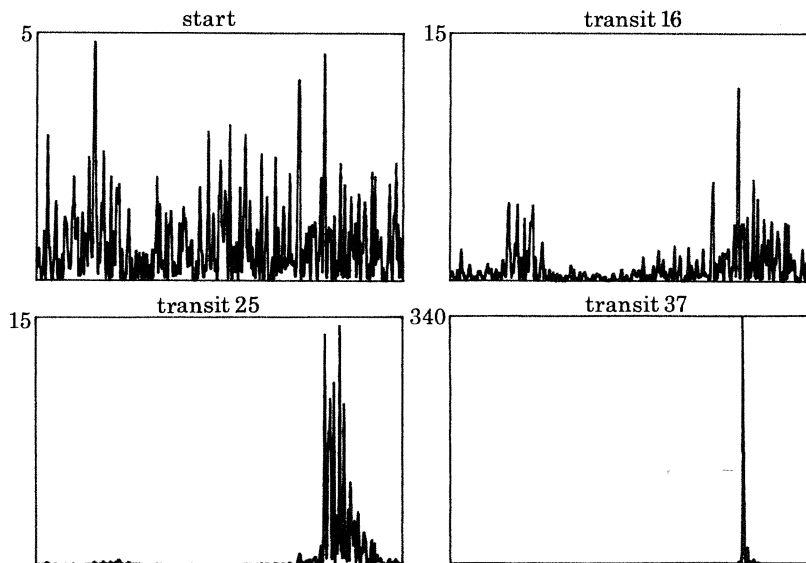


FIGURE 9. Computer simulation of the complete mode-locking process in a passively mode-locked quasi-continuous laser (New & Rea 1976). The arbitrary unit value on the top line of each frame indicates scale changes from frame to frame.

5. CONCLUSION

Simple rate equation models describing the essential features of the passive mode-locking process have been outlined. Depletion (or saturation) of the laser gain has been shown to play a vital role in both giant-pulse and quasi-continuous systems. In the former, the saturable absorber is entirely responsible for the pulse selection, although gain depletion aids the absorber indirectly by slowing the growth of the competing fluctuations at the critical stage of their development. For quasi-continuous systems, on the other hand, saturable amplification plays a direct part in the pulse selection and compression, and has a closely equivalent status to that of the saturable absorber in the mode-locking process.

REFERENCES (New)

- Ausschnitt, C. P. 1977 *IEEE J. Quantum Electron.* **QE-13**, 321–333.
 Bradley, D. J., Durrant, A. J. F., O'Neill, F. & Sutherland, B. 1969 *Physics Lett. A* **30**, 535–536.
 Caruso, A., Gratton, R. & Seka, W. 1973 *IEEE J. Quantum Electron.* **QE-9**, 1039–1043.
 Chan, C. K. & Sari, S. O. 1974 *Appl. Phys. Lett.* **25**, 403–406.
 Chekalin, S. V., Kriukov, P. G., Matveetz, Y. A. & Shatberashvili, O. B. 1974 *Opto-Electron.* **6**, 249–261.
 Creighton, J. R. & Jackson, J. L. 1971 *J. appl. Phys.* **42**, 3409–3414.
 Diels, J.-C., Van Stryland, E. & Benedict, G. 1978 *Optics Commun.* **25**, 93–96.
 Ferguson, A. I., Eckstein, J. N. & Hansch, T. W. 1978 *J. appl. Phys.* **49**, 5389–5391.
 Frigo, N. J., Daly, T. & Mahr, H. 1977 *IEEE J. Quantum Electron.* **QE-13**, 101–109.
 Garside, B. K. & Lim, T. K. 1973 *J. appl. Phys.* **44**, 2335–2342.
 Glenn, W. H. 1975 *IEEE J. Quantum Electron.* **QE-11**, 8–17.
 Haus, H. A. 1975a *IEEE J. Quantum Electron.* **QE-11**, 323–330.
 Haus, H. A. 1975b *J. appl. Phys.* **46**, 3049–3058.
 Haus, H. A. 1975c *IEEE J. Quantum Electron.* **QE-11**, 736–746.

- Heritage, J. P. & Jain R. K. 1978 *Appl. Phys. Lett.* **32**, 101–103.
- Ippen, E. P., Shank, C. V. & Dienes, A. 1972 *Appl. Phys. Lett.* **21**, 348–350.
- Kishida, S. & Yamane, T. 1976 *Optics Commun.* **18**, 19–20.
- Kryukov, P. G. & Letokhov, V. S. 1972 *IEEE J. Quantum Electron.* **QE-8**, 766–782.
- Lariontsev, E. G. & Serkin, V. N. 1974 *Radiophys. Quantum Electron.* **17**, 512–514 (translated from *Izv. vjssh. ucheb. Zaved. Radiofiz.* **17**, 679–682).
- Laser Focus* 1977 (July issue) **13**, 34–35.
- New, G. H. C. 1974 *IEEE J. Quantum Electron.* **QE-10**, 115–124.
- New, G. H. C. 1978 *IEEE J. Quantum Electron.* **QE-14**, 642–645.
- New, G. H. C. 1979 *Proc. Inst. elect. Electron. Engrs.* **67**, 380–397.
- New, G. H. C. & O'Hare, T. B. 1978 *Physics Lett. A* **68**, 27–28.
- New, G. H. C. & Rea, D. H. 1976 *J. appl. Phys.* **47**, 3107–3115.
- New, G. H. C., Orkney, K. E. & Nock, M. J. W. 1976 *Opt. & Quantum Electron.* **8**, 425–431.
- Risken, H. & Nummedal, K. 1968 *J. appl. Phys.* **39**, 4662–4672.
- Ruddock, I. S. & Bradley, D. J. 1976 *Appl. Phys. Lett.* **29**, 296–297.
- Seka, W. & Bunkenburg, J. 1978 *J. appl. Phys.* **49**, 2277–2280.
- Siegman, A. E. & Kuizenga, D. J. 1974 *Opto-Electron.* **6**, 43–66.
- Tomov, I. V., Fedosejevs, R. & Richardson, M. C. 1976 *Optics Commun.* **18**, 20.
- Tomov, I. V., Fedosejevs, R. & Richardson, M. C. 1977 *Appl. Phys. Lett.* **30**, 164–166.
- Wilbrandt, R. & Weber, H. 1975 *IEEE J. Quantum Electron.* **QE-11**, 186–190.
- Zel'dovich, B. Y. & Kuznetsova, T. I. 1972 *Soviet Phys. Usp.* **15**, 25–44 (translated from *Usp. fiz. Nauk* **106**, 47–84).